# Robust Adaptive Beamforming with SSMUSIC Performance Optimization in the Presence of Steering Vector Errors*

Biao Jiang, Qianliu Cheng, Guomin Ling
Lab of Sonar Syetem Research
Hangzhou Applied Acoustics Research Institute
Hangzhou, 310012, China
jbiao78@yahoo.com.cn

Journal of Digital Information Management



***ABSTRACT***: *A novel subspace projection approach was proposed to improve the robustness of adaptive beamforming and direction finding algorithms. The cost function of the signal subspace scaled multiple signal classification (SSMUSIC) is minimized in the uncertainty set of the signal steering vector, the optimal solution to the optimization problem is that the assumed steering vector can be modified as the weighed sum of the vectors orthogonally projected onto the signal subspace and the noise subspace. Using the estimated steering vector with small error to the true steering vector, the spectral peaks in the actual signal directions are guaranteed. Consequently, the problem of signal self-canceling encountered by adaptive beamforming due to steering vector mismatches is eliminated. Simulation and lake trial results show that the proposed method not only possesses high resolution performance, but also is robust to a few steering vector errors. Furthermore, the modified MUSIC algorithm outperforms the conventional MUSIC and SSMUSIC methods excellently.*

**Categories and Subject Descriptors**
**C. 3 [**Special purpose and application based systems**];** Signal Processing Systems **G.4 [Mathematicsl Software]**

**General Terms**
Signal processing, Signal Classification, Noise detection

**Keywords:** Robust adaptive beamforning, steering vector error, direction of arrival, diagonal loading, subspace projection matrix.

Received 30 November 2006; Revised 15 February 2007; Accepted 12 March 2007

## 1. Introduction

Multi-channel array signal processing has been widely and successfully used in radar, sonar, seismology, wireless communications, audio and speech processing, *etc*. Adaptive beamforming and high resolution direction-of-arrival (DOA) estimation algorithms have received much attention in the past a few decades, and among which, the minimum variance distortionless response (MVDR) [1] and multiple signal classification (MUSIC) algorithm [2] are the most popular two techniques.

Adaptive beamforming is utilized to enhance the signal of interest (SOI) corrupted in unwanted interferers and noises. In order to maximize the signal-to-interference-plus-noise-ratio (SINR) of the adaptive beamforming, the array steering vector of the SOI usually needs to be known precisely. It is well known that the MVDR method may suffer significant performance degradation even when there are very small array steering vector errors [3], which may result from many factors, e.g., signal local scattering, DOA mismatch, small number of data snapshots, nonstationary propagating environment, and individual sensor errors of positions, gains and phases, *etc*. The performance of adaptive beamforming is even worse when the SOI is contained in the training data snapshots. Therefore, robust beamforming has been a key issue in array applications when there are signal model errors.

The most widely used method to improve the robustness of adaptive beamforming is diagonal loading (DL), for its simplicity and effectiveness [1], [5]. The idea is to add a scaled identity matrix to the array covariance matrix prior to inversion, so that the norm of the weight vector and the white noise gain are constrained, and the noise eigenvalues are equalized. The key problem of DL method is how to choose the proper diagonal loading parameter [4]. Recently, some worst case performance optimization methods have been proposed to determine the DL value properly [6]–[8], by which the array output power is minimized subject to the constraint that the SOI with steering vectors lying in an uncertainty set not being suppressed, and hence, the output SINR is maximized when there are steering vector errors, and the robustness is improved. Besson *et.al* [9] had derived the theoretical SINR performance analysis of the generalized diagonal loading beamformers when existing random steering vector errors, it was pointed out in [9] that for higher uncertainties, the remedy to improve robustness must be to estimate the steering vector or to obtain additional information about the actual steering vector, rather than to preserve the array's response over a larger uncertainty ellipsoid.

Another popular robust method is the subspace-based beamformer or the projection approach [10], which uses the orthogonal projection of the presumed steering vector onto the signal-plus-interference subspace, instead of the presumed steering vector. The performance of the subspace-based beamformer is improved in most steering vector error cases, but this approach is limited to high signal-to-noise-ratio (SNR) scenarios and its performance depends on the low-rank stationary model of the training data.

MUSIC [2] algorithm is a subspace high-resolution DOA estimation method, and it has been proved that the standard MUSIC method possesses a certain degree of inherent robustness to steering vector errors [11]. However, for small training sample data size, low SNRs, or correlated signals, the estimated noise subspace (eigenspace) is poorly aligned with the true noise subspace, which may result in DOA's missing or spurious peaks occurring. To mitigate these shortcomings, a new subspace identification algorithm called SSMUSIC was proposed in [12], SSMUSIC seeks the local maxima by the ratio of two quadratic forms in the steering vector, scaling the MUSIC cost function by the estimated signal subspace to deal with subspace mismatches. Since SSMUSIC exploits more information of the true covariance matrix, it appears to be more robust to low SNRs and small data sets than MUSIC.

In this paper, we extend the SSMUSIC algorithm to a constrained optimization problem in the presence of steering vector errors, and the basic idea is that SSMUSIC or adaptive beamformer has a local maxima if the steering vector

* This work is partially supported by Chinese national defense project under contract 1010507010401.

coincides with the true signal response vector. The appropriate estimate of the steering vector can be found to maximize the SSMUSIC spectral function, or to minimize its reciprocal in the constrained uncertainty set of the steering vector. It is computationally effective and the performance improvement is obvious, and the proposed method can be considered as a generalized subspace projection approach.

The rest of this paper is organized as follows. Section 2 presents the signal model, and the SSMUSIC algorithm and adaptive beamfoming techniques are briefly reviewed. Section 3 proposes the new optimized robust adaptive beamforming algorithm based on SSMUSIC performance optimization criterion. Section 4 gives some numerical simulation results that illustrate the good behaviour of the proposed algorithm. Lake trial results are demonstrated in section 5, and section 6 concludes the paper.

## 2. Signal Model

Consider a uniform linear array (ULA) comprised of *M* sensors with element spacing *d*, the array output signal can be written as

$$\mathbf{x}(t) = \mathbf{a}(\theta_0)s_0(t) + \sum_{i=1}^{J}\mathbf{a}(\theta_i)s_i(t) + \mathbf{n}(t)$$

$$= \mathbf{As}(t)+\mathbf{n}(t)$$

$$= \mathbf{a}(\theta_o)s_o(t) + \mathbf{Bs}_i(t)+n(t) \quad (1)$$

where, $\mathbf{s}(t)$ is the source signal, $s_0(t)$ is the expected signal, $\mathbf{s}_i(t)$ is the $J\times1$ interference signal vector, $\mathbf{A}$ is the $M\times(J+1)$ signal-plus-interference steering matrix, $M\times J$ matrix $\mathbf{B}$ is the steering matrix of interferences, and $\mathbf{n}(t)$ denotes the additive Gaussian noise vector. The matrix $\mathbf{A}$ is as follows:

$\mathbf{A}=[\mathbf{a}(\theta_j), \mathbf{a}(\theta_1),...., \mathbf{a}(\theta_j)]$ , where $\mathbf{a}(\theta)$ is the array steering vector with *i*th element be expressed as , $\exp(j2\pi(i-1)d\sin\theta/\lambda)$, in which $\lambda$ is the propagating signal wavelength, then the array covariance matrix and its eigendecomposition can be written as

$$\mathbf{R} = E\{\mathbf{xx}^H\} = \mathbf{A}\mathbf{R}_s\mathbf{A}^H + \sigma^2\mathbf{I}$$

$$= \mathbf{U}\Lambda\mathbf{U}^H = \mathbf{U}_s\Lambda_s\mathbf{U}_s^H + \mathbf{U}_n\Lambda_n\mathbf{U}_n^H \quad (2)$$

where $\mathbf{U}_s$, $\mathbf{U}_n$ denote the eigenvector matrices of the signal and noise, respectively, and the diagonal elements of $\Lambda_s$, $\Lambda_n$ are the associated signal and noise eigenvalues. According to MUSIC algorithm, $\mathbf{A}$ and $\mathbf{U}_s$ span the same signal subspace, and the MUSIC cost function $g(\theta) = \mathbf{a}(\theta)^H U_n U_n^H \mathbf{a}(\theta)$ has a local minima in the actual direction of the incoming signal when the steering vector is exactly known. However, when there are steering vector errors, the minima may be away from the true signal direction, and the null may be not deep enough as to be distinguished.

SSMUSIC is an optional method to improve the performance of MUSIC [12], especially in low SNRs and short training data cases. The SSMUSIC cost function is given by

$$f(\theta) = \mathbf{a}^H(\theta)\mathbf{P}_n\mathbf{a}(\theta)/\left(\mathbf{a}^H(\theta)\mathbf{R}_A^+\mathbf{a}(\theta)\right) \quad (3)$$

where the numerator of $f(\theta)$ is the familiar MUSIC cost function which measures the energy that resolves in the noise subspace, and the denominator is a bearing response function that resolves finer scale information about the signal subspace. Thus SSMUSIC shows some robustness to the subspace mismatches since it exploits the full structure of the array spatial covariance matrix. And $\mathbf{P}_n=\mathbf{U}_n\mathbf{U}_n^H$ is the orthogonal projection matrix onto the noise subspace. $\mathbf{R}_A^+$ is the pseudo inverse of the signal covariance matrix $\mathbf{R}_A$. $\mathbf{R}_A$ and $\mathbf{R}_A^+$ are given by [12]:

$$\mathbf{R}_A = \mathbf{R} - \sigma_n^2\mathbf{I} = \mathbf{A}\mathbf{R}_s\mathbf{A}^H$$

$$= \mathbf{U}_s(\Lambda_s - \sigma_n^2\mathbf{I})\mathbf{U}_s^H \quad (4)$$

$$\mathbf{R}_A^+ = \mathbf{U}_s(\Lambda_S - \sigma_n^2\mathbf{I})^{-1}\mathbf{U}_s^H . \quad (5)$$

In practice, the exact covariance matrix $\mathbf{R}$ is unavailable. Therefore, the sample covariance matrix (SCM) estimated from *N* data snapshots

$$\mathbf{R} = \frac{1}{N}\sum_{i=1}^{N}\mathbf{X}(t)\mathbf{X}^H(t). \quad (6)$$

is used instead of $\mathbf{R}$. In theory, $\hat{\mathbf{R}}$ is a consistent estimator of $\mathbf{R}$, in other words, it converges in probability to $\mathbf{R}$ [14]. Thus, (5) is replaced by:

$$\mathbf{R}_A^+ = \hat{\mathbf{U}}_s(\hat{\Lambda}_s - \hat{\sigma}_n^2\mathbf{I})^{-1}\hat{\mathbf{U}}_S^H ,$$

with

$$\hat{\mathbf{R}} = \hat{\mathbf{U}}_s\hat{\Lambda}_s\hat{\mathbf{U}}_s^H + \hat{\mathbf{U}}_n\hat{\Lambda}_n\hat{\mathbf{U}}_n^H$$

$$\hat{\sigma}_n = \frac{1}{M-J-1}\sum_{i=J+2}^{M}\hat{\lambda}_i$$

where $\lambda$ is the eigenvalues of $\hat{\mathbf{R}}$ .

Perhaps the MVDR algorithm is the most commonly used adaptive beamforming, it is a spatial filter intending to make the output power minimized with the constraint that its response is equal to unity in the SOI direction. The MVDR criterion can be expressed as [1]:

$$\min_{\mathbf{w}}\mathbf{w}^H\hat{\mathbf{R}}\mathbf{w} \text{ s.t. (subject to) } \mathbf{w}^H\mathbf{a}(\theta_0) = 1 \quad (7)$$

Using the Lagrange multiplier method, the solution of (7) is given by

$$\mathbf{w}_{MV} = \frac{\hat{\mathbf{R}}^{-1}\mathbf{a}(\theta_0)}{\mathbf{a}^H(\theta_0)\hat{\mathbf{R}}^{-1}\mathbf{a}(\theta_0)} \quad (8)$$

(8) is also referred to as sample matrix inversion (SMI) technique. The number *N* of data snapshots is required to be larger than the number *M* of sensors, so that the SCM is invertible. In order to obtain an average output SINR within 3dB of that of the optimum one, *N* is needed to satisfy that, $N \geq 2M$ [13]. To combat the finite sample size effects and other random steering vector errors, the classical MVDR solution (8) is modified by adding a positive real factor *á* to the diagonal entries of the SCM, i.e., diagonal loading:

$$\mathbf{w}_{DL} = \frac{(\hat{\mathbf{R}}+\alpha\mathbf{I})^{-1}\mathbf{a}(\theta_0)}{\mathbf{a}^H(\theta_0)(\hat{\mathbf{R}}+\alpha\mathbf{I})^{-1}\mathbf{a}(\theta_0)} \quad (9)$$

where $\alpha$ is the diagonal loading factor.

The robust beamforming algorithms proposed in [6]–[8] can be regarded as generalized diagonal loading methods. The beamforming constraint condition is that the beamformer's

response be a little above unity for steering vectors that lie in an uncertainty ellipsoid being centered around the presumed steering vector. The corresponding worst case performance optimized solution is given by [9]

$$\mathbf{w}_{\mathrm{ADL}} = \frac{(\hat{\mathbf{R}}+\mathrm{Q})^{-1}\mathbf{a}}{\mathbf{a}^{H}(\hat{\mathbf{R}}+\mathrm{Q})^{-1}\mathbf{a}} \qquad (10)$$

where Q is the generalized diagonal loading matrix, and ADL represents adaptive diagonal loading. When the ellipsoid is a sphere, (10) is reduced to (9). To model the uncertainty ellipsoid is very complex as in [8], and from the results in [6], the performance of the robust Capon beamforming (RCB) with ellipsoid constraint is not better than that of the RCB with sphere constraint. So only the sphere constraint on the steering vector will be considered in this paper.

## 3. Proposed Robust Beamforming with SSMUSIC Performance Optimization

In [11], the MUSIC algorithm was extended to a constrained minimization problem when there existing steering vector errors, and it was shown that the extended MUSIC can't provide better DOA estimates than the standard MUSIC, but it has some robustness, i.e., there is a tradeoff between the robustness and the performance of the estimation bias and variance. Below, we'll generalize an extended SSMUSIC algorithm and apply its results to adaptive beamforming, in order to obtain robustness against the steering vector errors.

### 3.1 Constrainedly Optimized SSMUSIC Algorithm

When the signal steering vector is exactly known, the SSMUSIC can achieve better resolution than standard MUSIC algorithm, especially in low sample size scenarios [12]. Now let the assumed steering vector and the true steering vector be ($\varepsilon > \theta$) and $\tilde{\mathbf{a}}(\theta)$, when there are steering vector errors, the norm of the steering vector error can be bounded by a known : □ ≥

$$\|\tilde{\mathbf{a}} - \mathbf{a}\|^2 \le \varepsilon \qquad (11)$$

When the actual signal steering vector belongs to the uncertainty set (11), the SSMUSIC cost function must has a minima along the steering vector, so the robust SSMUSIC algorithm can be written as a constrained minimization problem as follows:

$$\min_{\tilde{\mathbf{a}}} f(\theta) = \tilde{\mathbf{a}}^{H}(\theta)\mathbf{P}_{\mathbf{n}}\tilde{\mathbf{a}}(\theta) / \left(\tilde{\mathbf{a}}^{H}(\theta)\mathbf{R}_{\mathbf{A}}{}^{+}\tilde{\mathbf{a}}(\theta)\right)$$

$$\text{s.t.} \quad \|\tilde{\mathbf{a}} - \mathbf{a}\|^2 \le \varepsilon \ . \qquad (12)$$

Using the fact that $\mathbf{U}_s\mathbf{U}_s^{H} + \mathbf{U}_n\mathbf{U}_n^{H} = \mathbf{I}$, with **I** the identity matrix. We can write

$$\tilde{\mathbf{a}} = \mathbf{U}_s\mathbf{U}_s^{H}\tilde{\mathbf{a}} + \mathbf{U}_n\mathbf{U}_n^{H}\tilde{\mathbf{a}} = \mathbf{U}_s\boldsymbol{\beta} + \mathbf{U}_n\boldsymbol{\gamma} \qquad (13)$$

where $\boldsymbol{\beta} = \mathbf{U}_s^{H}\tilde{\mathbf{a}}$, $\boldsymbol{\gamma} = \mathbf{U}_n^{H}\tilde{\mathbf{a}}$, and $f(\theta)$ can be rewritten as

$$f(\theta) = \|\boldsymbol{\gamma}\|^2 / \left\|(\boldsymbol{\Lambda}_s - \sigma_n^2\mathbf{I})^{-1/2}\boldsymbol{\beta}\right\|^2 \qquad (14)$$

Inserting (13) in (12) leads to the new constraint condition:

$$\|\tilde{\mathbf{a}} - \mathbf{a}\|^2 = \left\|[\mathbf{U}_s \quad \mathbf{U}_n]\begin{bmatrix}\boldsymbol{\beta}\\ \boldsymbol{\gamma}\end{bmatrix} - \mathbf{a}\right\|^2 = \left\|\begin{bmatrix}\boldsymbol{\beta}\\ \boldsymbol{\gamma}\end{bmatrix} - \begin{bmatrix}\mathbf{U}_s^{H}\\ \mathbf{U}_n^{H}\end{bmatrix}\mathbf{a}\right\|^2$$

$$= \left\|\boldsymbol{\beta} - \mathbf{U}_s{}^{H}\mathbf{a}\right\|^2 + \left\|\boldsymbol{\gamma} - \mathbf{U}_n{}^{H}\mathbf{a}\right\|^2 \le \varepsilon \qquad (15)$$

Since the denominator of $f(\theta)$ only influences the amplitude, the signal DOA is mainly determined by the nulls of *f*, i.e. the zeros of the numerator. The vector $\boldsymbol{\beta}$ is taken as $\hat{\boldsymbol{\beta}} = \lambda_1\mathbf{U}_s{}^{H}\mathbf{a}$, thus the optimized solution of $\boldsymbol{\gamma}$ is $\hat{\boldsymbol{\gamma}} = \lambda_2\mathbf{U}_n{}^{H}\mathbf{a}$, $\boldsymbol{\gamma}$ can't comprise one component which is perpendicular to $\mathbf{U}_n{}^{H}\mathbf{a}$. Otherwise, the value of $f(\theta)$ will increase and the constraint set will decrease, which is the same phenomenon as in [11]. Using $\hat{\boldsymbol{\beta}}$ and $\hat{\boldsymbol{\gamma}}$ in (14), the minimization problem of (12) is reformulated as

$$\min_{\lambda_1,\lambda_2} \frac{\|\lambda_2\|^2\|\mathbf{U}_n{}^{H}\mathbf{a}\|^2}{\|\lambda_1\|^2|\mathbf{a}^{H}(\theta)\mathbf{R}_{\mathbf{A}}{}^{+}\mathbf{a}(\theta)|^2} = \min_{\lambda_1,\lambda_2} \frac{\|\lambda_2\|^2}{\|\lambda_1\|^2}$$

$$\text{s.t.} \ \left|1-\lambda_1\right|^2\left\|\mathbf{U}_s{}^{H}\mathbf{a}\right\|^2 + \left|1-\lambda_2\right|^2\left\|\mathbf{U}_n{}^{H}\mathbf{a}\right\|^2 \le \varepsilon \qquad (16)$$

It is obvious that $\lambda_1$ and $\lambda_2$ are confined to an ellipse centered at coordinate (1,1) as shown in Figure 1, and the half-lengths of the elliptical axes are $\varepsilon^{1/2} / \left\|\mathbf{U}_s{}^{H}\mathbf{a}\right\|$ and $\varepsilon^{1/2} / \left\|\mathbf{U}_n{}^{H}\mathbf{a}\right\|$, respectively.

Observing the geometrical relationship between $\lambda_1$ and $\lambda_2$, it can be concluded that the solution of problem (16) is

$$\hat{\lambda}_1 = 1 + \varepsilon^{1/2} / \left\|\mathbf{U}_s{}^{H}\mathbf{a}\right\| \ ,$$

$$\hat{\lambda}_2 = 1 - \varepsilon^{1/2} / \left\|\mathbf{U}_n{}^{H}\mathbf{a}\right\| \qquad (17)$$

for $\varepsilon < \left\|\mathbf{U}_n{}^{H}\mathbf{a}\right\|^2$, whereas when $\varepsilon \ge \left\|\mathbf{U}_n{}^{H}\mathbf{a}\right\|^2$, the solution of (16) is $\hat{\lambda}_2 = 0$, and it is obvious to see that $\hat{\lambda}_1$ can be chosen arbitrarily.

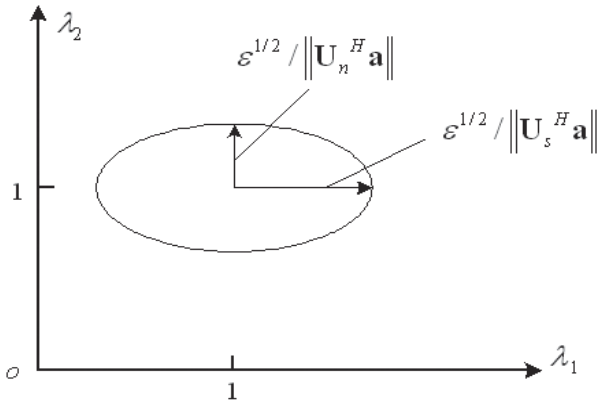


Figure 1. Constrained ellipse of $\ddot{e}_1$ and $\ddot{e}_2$

Using (17) in (13), the approximation to the actual steering vector $\tilde{\mathbf{a}}(\theta)$ can be estimated by:

$$\hat{\tilde{\mathbf{a}}} = \begin{cases} \hat{\lambda}_1\mathbf{U}_s\mathbf{U}_s^{H}\mathbf{a} + \hat{\lambda}_2\mathbf{U}_n\mathbf{U}_n^{H}\mathbf{a} & \varepsilon < \left\|\mathbf{U}_n^{H}\mathbf{a}\right\|^2 \\ \mathbf{U}_s\mathbf{U}_s^{H}\mathbf{a} & \varepsilon \ge \left\|\mathbf{U}_n^{H}\mathbf{a}\right\|^2 \end{cases} \qquad (18)$$

To maintain the modulus of the estimated vector $\hat{\tilde{\mathbf{a}}}$ be constant to be *M*, which is the modulus of the assumed steering vector **a**, is scaled to

$$\hat{\mathbf{a}} = \hat{\mathbf{a}}\sqrt{M}/\left\|\hat{\mathbf{a}}\right\| \qquad (19)$$

The advantage of the scaling operation is that the signal power estimate can be less biased, it's because that the array weight vector has the "scaling ambiguity" [6], i.e., $\mathbf{w}^H\mathbf{a}=(1/\alpha)\mathbf{w}^H(\alpha\,\mathbf{a})$, with **w** the adaptive weight vector to maintain the signal undistortionless for MVDR beamforming.

Form (18), we can see that the steering vector estimate is the weighted sum of the projection of the presumed steering vector **a** onto the signal plus interference subspace and the noise subspace, respectively. Thus, the proposed method can be considered as a generalized projection approach, which is more robust to the steering vector errors since it exploits more eigen-structure information.

Using (19) instead of the presumed steering vector **a**, the robust SSMUSIC spatial spectral function is given by

$$\text{fH-SSMUSIC}(\theta) = (\hat{\hat{\mathbf{a}}}^H(\theta)\mathbf{R}_A + \hat{\hat{\mathbf{a}}}(\theta))/\hat{\hat{\mathbf{a}}}^H(\theta)\mathbf{P}_n\hat{\hat{\mathbf{a}}}(\theta), \qquad (20)$$

which is the reciprocal of the cost function in (12).

### 3.2 Robust Eigenspace-based Beamforming

The proposed robust eigenspace-based beamforming is to using (19) instead of the presumed steering vector **a** in the MVDR weight vector (8):

$$\mathbf{w}_{\text{R-ES}} = \hat{\mathbf{R}}^{-1}\hat{\mathbf{a}}/(\hat{\mathbf{a}}^H\hat{\mathbf{R}}^{-1}\hat{\mathbf{a}}) \qquad (21)$$

## 4. Numerical Results

An 8-element uniform linear array with 1m interelement spacing, which is half-wavelength of the received narrowband signal with center frequency 750Hz, is considered here. The underwater sound speed is assumed to be $c$=1500m/s. The received noise is modelled as additive temporal Gaussian white noise with power 0dB. There are two uncorrelated narrowband sources impinging on the array from $\theta_1$=0° and $\theta_2$=20° relative to the array broadside, respectively. The 0° signal is the expected signal and the 20° signal is assumed to be the interference. Three algorithms are compared: MVDR, diagonal loaded MVDR (LMVDR) and the proposed robust eigenspace-based adaptive beamforming (R-ES). For the LMVDR algorithm, the DL factor $\alpha$ is 10 (i.e. 10dB relative to the background noise). The array output SINRs are obtained by averaging 100 independent realizations.

### 4.1 Beam Directivity Comparison

The SNRs of the two signals are set to be 5dB and 10dB. The number of data snapshots is $N$=200, and $\varepsilon$=0.6 for our proposed R-ES method. Figure 2 (a) shows the beampatterns of the three algorithms with no DOA mismatch, i.e., the array steering angle is 0°, in accordance with the actual signal direction. It can be seen that the MVDR method has a deeper null nearby the interference, but its sidelobe level is relatively higher, and the maximum response axis (MRA) is a little deviated from the actual source position. The performance of the proposed R-ES method is similar to that of the LMVDR but has a deeper null at the interference position.

Figure 2 (b) displays the corresponding beampatterns when there are DOA mismatch, in this example, the array is steered to 1°. In this case, the MVDR beamformer forms a null at the direction of the expected signal, because it is treated as a interference due to undistortionless response constraint in the direction of 1°. This is the so called "signal self-cancelling" for the adaptive weight try to make the output power minimized, which would suppress the useful signal. The contrary is that all the three algorithms have a null in the interference direction, this is also caused by the power minimization criterion for the interference direction is far away from the steering direction. Thus, small errors of the interferers' steering vectors have little effect on the beamformer's performance. The MRA of the R-ES method is still well steered to 0°, however, the LMVDR has a larger MRA deviation despite it has some robustness.

### 4.2 Spatial Spectra Comparison

In this example, the spatial spectra of the MVDR-like and MUSIC-like algorithms are compared, respectively.

Figure 3 is the normalized spectra of the MVDR-like algorithms. It can be seen that, for small steering vector errors, such as $\varepsilon$=0.06, the proposed R-ES method is reduced to the MVDR algorithm. But for larger $\varepsilon$, for example, $\varepsilon$=0.6, the R-ES has a wider spectral peaks near the signal DOA's, that is to say that the acceptance angle of the robust method is widened. Moreover, the output background noise level is much lower that that of the LMVDR's, and the resolution of LMVDR is dropped. We can adjust the parameter $\delta$ by a tradeoff between the high-resolution capability and the robustness.

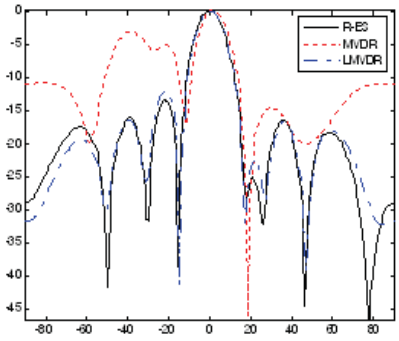


(a) no DOA mismatch

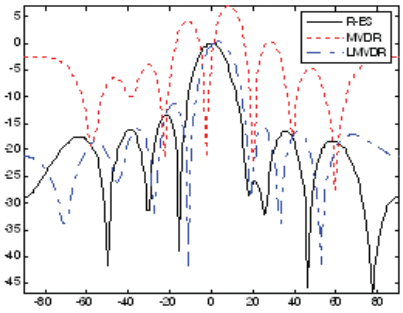


(b) 1° DOA mismatch

Figure 2. Beampatterns comparison with or without DOA mismatch

Figure 4 demonstrates the superior performance of the proposed robust method relative to MUSIC and SSMUSIC. The R-ES method has super-low sidelobes, and super-directivity for small $\varepsilon$. Similar to those in Figure 3, the width of the spectral peak is increasing as $\varepsilon$ is increasing, which shows the robustness to the steering vector errors. Furthermore, The R-ES method not only has robustness, but also maintains high-resolution seeing the keen-edged peaks. SSMUSIC has a lower sidelobe than MUSIC, but its resolution is somewhat decreased. The MUSIC method has the highest sidelobe level.

Now we consider that the array is suffered from shape distortion, i.e. element position perturbations, which is common in towed sonar applications. The position perturbations of *M* elements is assumed to be independently, and identically distributed (i.i.d) random variables, and mutually uncorrelated each other. Then the coordinate of the *i*th element position at the *n*th snapshot can be written as

$$(x_i(n), y_i(n)) = ((i-1)d + \Delta x_i(n), \Delta y_i(n)) \quad (22)$$

where $\Delta x_i(n)$, $\Delta y_i(n)$ are random Gaussian processes with equal variance, and the standard deviation in this example is assumed to be 0.08m, which is one percentage of 12.5 wavelengths. Figure 5 (a) shows the DOA estimation root-mean-square-errors (RMSEs) versus input SNR for 0° source, the two sources have equal power, $\varepsilon$ =0.6 is for the R-ES method. The stochastic Cramér-Rao bound (CRB) [15] of the bearing estimation is also depicted, which is given by

$$\mathrm{CRB}(\theta) = \frac{\sigma_n^2}{2N}\left\{\mathrm{Re}(\mathbf{D}^H\Pi_A^{\perp}\mathbf{D}) \odot (\hat{\mathbf{R}}_s\mathbf{A}^H\hat{\mathbf{R}}^{-1}\mathbf{A}\hat{\mathbf{R}}_s)^T\right\}^{-1} \quad (23)$$

where **D** is the derivative matrix of **A** with respect to $\theta$, $\Pi_{\mathbf{A}}^{\perp}$ is the orthogonal projection matrix onto the complementary subspace of **A**:

$$\Pi_{\mathbf{A}}^{\perp} = \mathbf{I} - \mathbf{A}(\mathbf{A}^H\mathbf{A})^{-1}\mathbf{A}^H, \quad (24)$$

and ⊙ denotes the Hardmard-Schur product, Re(·) the real part. It's clear to see the performance improvements of the R-ES algorithm under shape distortion condition.

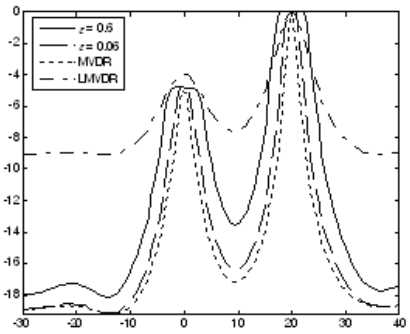


Figure 3. Spatial spectra of MVDR-like algorithms

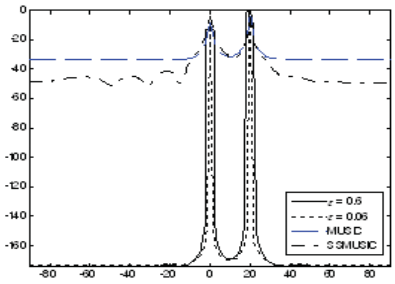


Figure 4. Spatial spectra of MUSIC-like algorithms

For comparison, Figure 5 (b) shows the corresponding RMSEs of the 0° source versus SNR without array shape distortion, the performances of the R-ES method and MUSIC method are similar, which is a little better than that of the SSMUSIC algorithm in low SNR scenarios, such as when SNR is below –10dB, and when the SNR of the received signal is larger than –7.5dB, the estimation RMSE of R-ES method is dropped quickly, even below the CRB value. If the 5 (b), steering vector errors bounding parameter $\varepsilon$ is fixed when SNR is changing, the RMSE would not drop any more, from Figure the curve is fluctuating around –35dB, and it will be larger than the CRB value again when the input SNR reaches a certain even larger threshold.

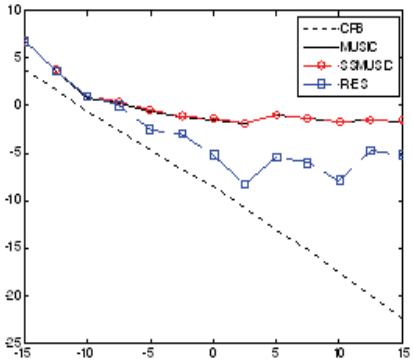


(a) with array shape distortion

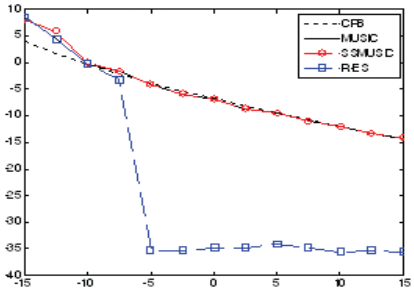


(b) without array shape distortion

Figure 5. DOA estimation RMSEs of the 0° source vs. SNR

### 4.3 SINR Performance for DOA Mismatch Error Case

Besides the beam directivity, another important measure of the beamformer performance is the SINR, which is given by

$$\mathrm{SINR} = \frac{\sigma_s^2 \left|\mathbf{w}^H\mathbf{a}_s\right|^2}{\mathbf{w}^H\hat{\mathbf{R}}_{i+n}\mathbf{w}} \quad (25)$$

where $\sigma_s^2$ is the interested signal power, and $\mathbf{a}_s$ is the corresponding steering vector. $\hat{\mathbf{R}}_{i+n}$ is the sample covariance matrix of the interference-plus-noise.

Using the interested signal-free snapshots, we can get the "optimal" weight vector and the "optimal" SINR. The optimal weight vector $\mathbf{w}_{\mathrm{opt}}$ is given by

$$\mathbf{W}_{\mathrm{opt}} = \hat{\mathbf{R}}_{i+n}^{-1}\hat{\mathbf{a}} / (\hat{\mathbf{a}}^H\hat{\mathbf{R}}_{i+n}^{-1}\hat{\mathbf{a}}) \quad (26)$$

Thus, using (26) in (25), we can derive the optimal output SINR as follows:

$$\mathrm{SINR}_{\mathrm{opt}} = \sigma_s^2\mathbf{a}_s^H\hat{\mathbf{R}}_{i+n}^{-1}\mathbf{a}_s \quad (27)$$

Figure 6 depicts the output SINRs versus SNR when there are no DOA mismatch and 2° DOA mismatch by 100 independent Monte-Carlo experiments, respectively. From Figure 6 (a), the SINR of R-ES is nearly identical to that of the LMVDR's with no DOA mismatch, and the SINR of MVDR is increasing with the input SNR. However, even small DOA mismatches can cause great performance degradation for conventional MVDR method as shown in Figure 6 (b), and in this case, the proposed R-ES method outperforms LMVDR for the improper chosen loading value, and the loading value is not varying with the SNR and the steering vector errors. The SINR of the proposed R-ES approaches the optimal.

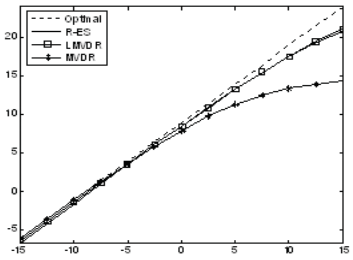


(a) no DOA mismatch

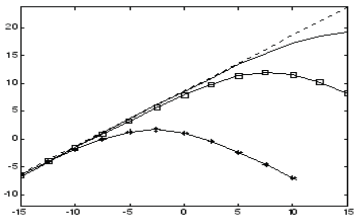

(b) 2° DOA mismatch)

Figure 6. Output SINR vs. SNR

Figure 7 shows the array SINR curves versus the number of snapshots with no DOA mismatch and 2° DOA mismatch, respectively. The parameter $\varepsilon$ is 0.6. Without DOA mismatch, the asymptotic (large snapshots *N*) performances of R-ES and LMVDR are similar, and they are much better than that of MVDR's, as shown in Figure 7 (a). However, when there are 2° small DOA mismatch, approximately 2dB SINR improvement is achieved using R-ES method than LMVDR at the stable state in Figure 7 (b), and the MVDR method is asymptotically less inefficient, whose SINR is about 11dB less than that of R-ES method.

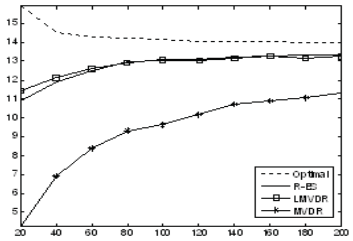


(a) no DOA mismatch

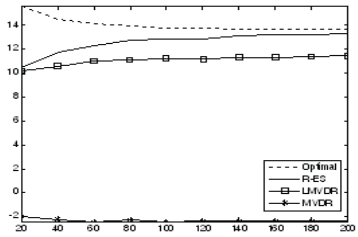


(b) 2° DOA mismatch

Figure 7. Output SINR vs. snapshots

### 4.4 Performance vs. DOA Mismatch

In this example, we'll examine the algorithm performance as the DOA mismatch is changing. Figure 8 demonstrates the output SINR curves when the value of the DOA mismatch is varying from –8° to 8°, the SINR of MVDR decreases quickly when the mismatch is increasing, LMVDR shows some better performance than MVDR, and a little performance degradation starts occurring when the DOA mismatch being larger than 4° for the optimal beamformer that using the signal-free snapshots. However, interestingly and wonderfully, our proposed method maintains the constant optimal SINR value among the total mismatched array steering angle area ranging from –8° to 8°, the best robustness is obtained.

### 4.5 SINR Performance for Local Scattering Case

This example corresponds to the scenario where the received signal of interest is distorted by local scattering effects, e.g. active sonar targets reflected signals, multipath wireless propagating environment. The coherent local scattering signal steering vector can be written as in [9]:

$$\tilde{\mathbf{a}} = \mathbf{a} + \frac{1}{\sqrt{L}} \sum_{k=1}^{L} g_k \mathbf{b}(\tilde{\theta}_k) \qquad (28)$$

$\mathbf{b}(\theta)$ represents the steering vector of a plane wave arriving from $\theta$, *L* is the number of scattering paths, and $g_k$ is zero-mean, i.i.d. random variable with power $\sigma_g^2$. According to (28), the covariance matrix of the steering vector errors can be written as

$$\begin{aligned} \mathbf{C}_a &= E\{(\hat{\tilde{\mathbf{a}}} \cdot \mathbf{a})\,(\hat{\tilde{\mathbf{a}}} \cdot \mathbf{a})\,H\} \\ &= \sigma_g^2 \int_{\tilde{\theta}} p(\tilde{\theta}) \mathbf{b}(\tilde{\theta}) \mathbf{b}^H(\tilde{\theta}) d\tilde{\theta} \end{aligned} \qquad (29)$$

where $p(\tilde{\theta})$ is the probability density function (pdf) of $\tilde{\theta}$, the frequent ly used pdf models are uniform and Gaussian distributions, which are given as follows, respectively:

$$p_u(\tilde{\theta}, \sigma_\theta) = \begin{cases} 1/2\sigma_\theta & |\tilde{\theta} - \theta| \le \sigma_\theta \\ 0 & \text{otherwise} \end{cases} \qquad (30)$$

$$p_g(\tilde{\theta}, \sigma_\theta) = \frac{1}{\sqrt{2\pi}\sigma_\theta} \exp\left(-\frac{(\tilde{\theta} - \theta)^2}{2\sigma_\theta^2}\right) \qquad (31)$$

where the subscript "*u*" means the uniform distribution, and "*g*" means the Gaussian distribution. $\theta$ is the normal arriving angle or central angle, $\sigma\theta$ is the standard deviation of the scattering angular spread.

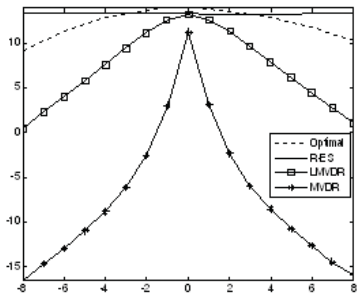


Figure 8. Output SINR vs. SNR (2° DOA mismatch)

For small deviation $\sigma\theta$, we have

$$\sin(\theta + \tilde{\theta}) \approx \sin\theta + \tilde{\theta}\cos\theta \qquad (32)$$

Using (30)–(32), and by some arithmetic manipulations, the *k*,*l*th ($1 \le k,l \le M$) element of (29) can be derived as

$$[\mathbf{C}_a^u]_{kl} = \sigma_g^2 \exp(j\phi\sin\theta)\,\mathrm{sinc}(\phi\cos\theta\sigma_\theta) \qquad (33)$$

$$[\mathbf{C}_a^g]_{kl} = \sigma_g^2 \exp(j\phi\sin\theta)\exp[-(\phi\cos\theta\sigma_\theta)^2/2]\,, \qquad (34)$$

$$\phi = 2\pi f(k-l)d/c$$

sinc $(x) = \sin x / x$.

(29) can also be written in matrix form:

$$\mathbf{C}_a^u = (\mathbf{a}(\theta)\mathbf{a}^H(\theta)) \odot \tilde{\mathbf{C}}_a^u \qquad (35)$$

$$C_a^g = (a(\theta)a^H(\theta)) \odot \breve{C}_a^g \quad (36)$$

with

$$[\breve{C}_a^u]_{kl} = \sigma_g^2 \mathrm{sinc}(\phi \cos\theta \sigma_\theta)$$

.

$$[\breve{C}_a^g]_{kl} = \sigma_g^2 \exp[-(\phi \cos\theta \sigma_\theta)^2/2]$$

Therefore, the scattered signal steering vector for small angular spread is given by

$$\tilde{\mathbf{a}} = \mathbf{a} + \mathbf{C}_a^{1/2}\mathbf{u} \quad (37)$$

where **u** is the zero-mean, unit-variance circular complex Gaussian vector.

The corresponding SINR for local scattering scenarios is given by

$$\mathrm{SINR} = \frac{\sigma_s^2 E_{\mathbf{a}}\left(|\mathbf{w}^H\mathbf{a}|^2\right)}{\mathbf{w}^H\hat{\mathbf{R}}_{i+n}\mathbf{w}} = \frac{\sigma_s^2\mathbf{w}^H(\mathbf{a}\mathbf{a}^H + \mathbf{C}_a)\mathbf{w}}{\mathbf{w}^H\hat{\mathbf{R}}_{i+n}\mathbf{w}} \quad (38)$$

where $E_a$ denotes the expectation with respect to the pdf of vector **a**, and using (27), the averaging optimal SINR is given as follows:

$$\mathrm{SINR}_{\mathrm{opt}} = \int_{\mathbf{a}} \sigma_s^2 \tilde{\mathbf{a}}^H \hat{\mathbf{R}}_{i+n}^{-1} \tilde{\mathbf{a}} p(\mathbf{a}) d\mathbf{a}$$

$$= \sigma_s^2 \int_{\mathbf{a}} \mathrm{Tr}\left(\hat{\mathbf{R}}_{i+n}^{-1}(\tilde{\mathbf{a}}\tilde{\mathbf{a}}^H)\right) p(\mathbf{a}) d\mathbf{a} = \sigma_s^2 \mathrm{Tr}\left(\hat{\mathbf{R}}_{i+n}^{-1}(\mathbf{a}\mathbf{a}^H + \mathbf{C}_a)\right) \quad (39)$$

where Tr(·) denotes the matrix trace, $p$(**a**) is the pdf of **a**.

*Experimental conditions*: the interference signal from 20° is assumed to be a plane wave with interference-to-noise-ratio (INR)=20dB, but the signal of interest from 0° is a local scattered source with angular spread $\sigma_\theta$=2°, and the array steering direction is 2°, i.e., 2° DOA mismatch with the actual signal direction. Figure 9 shows the SINR curves of the optimal and adaptive beamforming evaluated by (38) and (39), and the SOI is uniform and Guassian angular spread, respectively. It's obvious to see the enhanced performance of the proposed R-ES approach, and the algorithm behaviors are similar under the two scattering scenarios.

Figure 10 displays the performance of the test methods versus the number of snapshots for the fixed sensor SNR=5dB, note that the SNR in this example is defined by taking into account only the direct arriving signal path, and the Gaussian angular spread source is considered here.

Figure 11 compares the output SINR of the test methods versus the DOA mismatch, which is changing from –8° to 8°, the R-ES method has the superior robustness against DOA mismatch and local scattering.

## 5. Lake Trial Results

In this section, the algorithm performances are compared using the towed sonar lake trial data. One narrowband source signal with 1kHz central frequency impinges on the line array, and 10 sensors are selected to perform adaptive beamforming. The snapshots are 1024, and the sampling frequency was 12kHz, and the parameter å is still chosen as 0.6, and the DL value of LMVDR is 10dB as before.

The spatial spectra of R-ES, LMVDR and MVDR algorithms are depicted in Figure 12, it is obvious that the R-ES method outperforms the other two, and the signal power is underes-

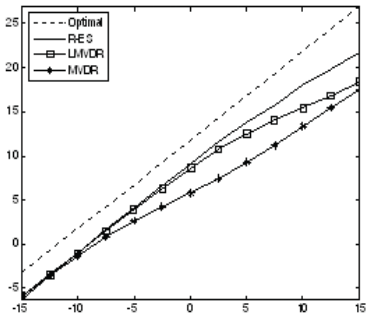


(a) uniform angular spread

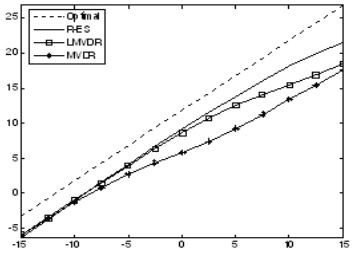


(b) Gaussian angular spread

Figure 9. Output SINR vs. SNR. Steered to 2°, $\sigma_\theta$=2°, INR=20dB, $\varepsilon$ = 0.6,

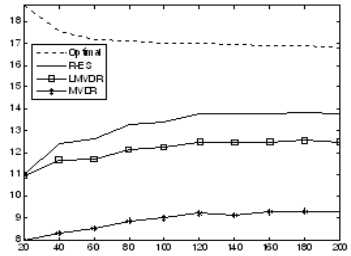


Figure 10. Output SINR vs. number of snapshots

Steered to 2°, $\sigma_\theta$=2°, INR=20dB $\varepsilon$ =0.6, Gaussian angular spread.

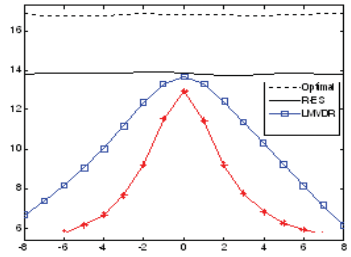


Figure 11. Output SINR vs. DOA mismatch.

s?=2°, INR=20dB, e= 0.6, Gaussian angular spread

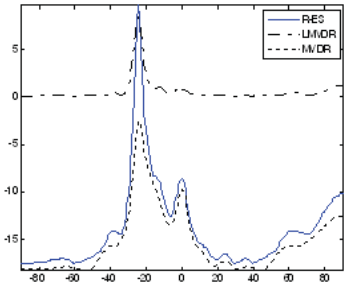


Figure 12. Lake trial result

timated by MVDR. The R-ES method has the highest resolution and the effective signal power estimate. The LMVDR method has higher background noise level due to the imprecise DL value. Since there are array shape distortions,

and sensor amplitude and phase errors in practice, our method is robust to a variety of steering vector errors from the lake trial result, and its performance is less sensitive to the robust parameter $\varepsilon$.

## 6. Conclusions

A novel eigenspace-based robust high-resolution array signal processing method is proposed based on the extended SSMUSIC subspace DOA estimation algorithm. This method effectively combines the spatial selectivity of adaptive beamforming with the super-resolution property of the subspace-based algorithm which has the inherent robustness. Theoretical analysis and numerical results have shown the performance improvements in beampattern, SINR, resolution and sensitivity to steering vector errors such as DOA mismatches, array shape distortions and local scattering. Furthermore, this method is computationally less complex and asymptotically efficient.

## References


[1] Cox, H., Zeskind, R.M., Owen, M.H (1987). Robust adaptive beamforming. *IEEE Trans. Acoust., Speech, Signal Processing*, 35 (10) 1365–1376.

[2] Schmidt, R. O (1986). Multiple emitter location and signal parameter estimation. *IEEE Trans. Antennas Propagat.*, 34 (3) 276–280.

[3] Er, M.H., Ng, B.C. (1994). A new approach to robust beamforming in the presence of steering vector errors. *IEEE Trans. Signal Processing,* 42 (7) 1826–1829.

[4] Gershman, A.B. (2003). Robust adaptive beamforming: an overview of recent trends and advances in the field. Proceedings of Int. Conf. on Antennas Theory and Tech, Sevastopal, Ukraine. 30–35.

[5] Trees, H.V. (2002). Optimum Array Processing. New York: Wiley. 505.

[6] Li, J., Stoica, P., Wang, Z. (2003). On robust Capon beamforming and diagonal loading. *IEEE Trans. Signal Process.,* 51(7), 1702–1715.

[7] Vorobyov, S., Gershman, A., Luo, Z (2003). Robust adaptive beamforming using worst-case performance optimization: a solution to the signal mismatch problem. *IEEE Trans. Signal Process.*, 51 (2) 313–324.

[8] Lorenz, R., Boyd, S (2003). Robust minimum variance beamforming. Proceedings of 37th Asilomar Conf. 1345–1352.

[9] Besson, O., Vincent, F (2005). Performance analysis of beamformers using generalized loading of the covariance matrix in the presence of random steering vector errors. *IEEE Trans. Signal Process*., 53 (2) 452–459.

[10] Feldman, D. D., Griffiths, L. J (1994). A projection approach to robust adaptive beamforming. *IEEE Trans. Signal Processing*, 42 (4) 867–876.

[11] Stoica, P., Wang, Z.S. Li, J (2005). Extended derivations of MUSIC in the presence of steering vector errors. *IEEE Trans. Signal Processing*, 53 (3) 1209–1211.

[12] McCloud, M.L., Scharf, L.L. (2002). A new subspace identification algorithm for high-resolution DOA estimation. *IEEE Trans. Antennas Propagat*., 50 (10) 1382–1390.

[13] Mestre, X., Lagunas, M.A (2006). Finite sample size effect on minimum variance beamformers: Optimum diagonal loading factors for large arrays. *IEEE Trans. Signal Process.*, 54 (1) 69–82.

[14] Morell, A., P.-Iserte, A., P.-Neira, A.I. (2005). Fuzzy inference based robust beamforming. *Signal Processing*, 85 (10) 2014–2049.

[15] Stoica, P., Nehorai, A (1989). MUSIC, Maximum likelihood, and Cramér–Rao bound. *IEEE Trans. Acoust., Speech, Signal Processing*, 37 (5) 720–741.